GEOMATICS AND ENVIRONMENTAL ENGINEERING • Volume 19 • Number 6 • 2025

https://doi.org/10.7494/geom.2025.19.6.75

Phunsap Thari[1], Chalermchon Satirapod[2]

Performance Assessment of Second-Generation SBAS Prototype in Thailand

Abstract: This study evaluates the preliminary performance of the dual-frequency multi-constellation satellite-based augmentation system (DFMC SBAS) prototype that was deployed in Thailand, focusing on key performance indicators such as positional accuracy and continuity. To this end, real data that was collected from 4, 8, and 12 ground tracking stations in Thailand was used to calculate SBAS corrections for the periods of January 1–7, April 1–7, August 1–7, and December 1–7, 2023. The accuracy of these corrections for single-point positioning was then tested using data from 20 continuously operating reference stations (CORS) in the region. The results showed that the correction data that was derived from the data from the 8 and 12 ground tracking stations significantly improved the efficiency of the single-point positioning, thus meeting the required standards for Category I (CAT-I) aviation operations. This initial assessment provides a solid foundation for the continued development of a fully operational DFMC SBAS that is tailored to Thailand's specific requirements.

Keywords: DFMC SBAS, CORS, CAT-I, Thailand

Received: May 13, 2025; accepted: August 21, 2025

© 2025 Author(s). This is an open-access publication, which can be used, distributed, and reproduced in any medium according to the Creative Commons CC-BY 4.0 License

[1] Chulalongkorn University, Faculty of Engineering, Department of Survey Engineering, Mapping and Positioning from Space (MAPS) Technology Research Center, Bangkok, Thailand, email: ohmtachi@gmail.com, https://orcid.org/0009-0006-8551-2524

[2] Chulalongkorn University, Faculty of Engineering, Department of Survey Engineering, Mapping and Positioning from Space (MAPS) Technology Research Center, Bangkok, Thailand, email: chalermchon.s@chula.ac.th (corresponding author), https://orcid.org/0000-0003-2932-0334

1. Introduction

The satellite-based augmentation system (SBAS) has proven to be a powerful tool in improving the efficiency and accuracy of global navigation satellite system (GNSS) surveying [1–3]. By providing real-time error corrections and broad geographic coverage, SBAS has significantly improved single-point positioning (SPP) and other GNSS applications, thus offering notable benefits for industries such as aviation and beyond [4–7]. The widespread adoption of first-generation SBAS systems, which include the European Geostationary Navigation Overlay Service (EGNOS), the Wide Area Augmentation System (WAAS), the GPS-aided GEO-Augmented Navigation System (GAGAN), the Multi-functional Transport Satellite Augmentation System (MSAS), and the BeiDou Satellite-Based Augmentation System (BDSBAS), reflects a global commitment toward improving navigation services, thus paving the way for more reliable and accurate satellite navigation [6, 8–15].

Although Thailand does not have its own SBAS infrastructure as of yet, it can still benefit from the services that are provided by neighboring systems such as GAGAN, SouthPAN, and BDSBAS. However, these external systems cannot significantly improve the positioning accuracy within Thailand, as the ionospheric error-correction data that they provide does not align with the specific geophysical conditions of the country [16–19]. This challenge is particularly pronounced, as Thailand's proximity to the equator makes it more vulnerable to ionospheric disturbances [20–26].

The advancement of GNSS has significantly improved the accuracy and precision of surveying [27–29]. This progress has been further supported by the expansion of SBAS. The introduction of second-generation SBAS – particularly, dual-frequency multi-constellation (DFMC) SBAS – has taken these improvements a step further. By providing L5 corrections, DFMC SBAS effectively mitigates ionospheric errors and is compatible with multiple GNSS constellations, including GPS, BeiDou (BDS), Galileo, and GLONASS. Through the simultaneous use of L1/CA and L5 signals, the system greatly improves both the positioning accuracy and service continuity, thereby optimizing the performances of GNSS-based applications [30–32].

Evaluations of second-generation SBAS enhancements in the Australian and Pacific regions have demonstrated that DFMC SBAS can reliably deliver integrity monitoring and high-precision positioning. Accuracy was consistently maintained within a submeter-to-meter range, and the protection levels remained within the predefined thresholds. These results highlighted the potential of the system to significantly improve satellite navigation services in the Asia-Pacific region – particularly in aviation and other safety-critical domains [33–35].

In parallel, the second-generation BeiDou Satellite-Based Augmentation System (BDSBAS) has also undergone substantial upgrades with the launch of a new satellite network, resulting in improved performance and reliability of the BeiDou Navigation Satellite System (BDS) [27, 36, 37]. The enhanced BDSBAS now supports DFMC operations, making it compatible with BDS, GPS, Galileo, and GLONASS.

This enables the system to offer more-flexible and more-resilient signal services. Preliminary assessments suggest that BDSBAS can achieve positioning accuracy within a submeter-to-meter range in its supported regions [29, 38–40]; however, its ability to improve the efficiency of GNSS surveying in Thailand is limited, as the country currently lies outside the coverage area of the BDSBAS network [14].

In 2022, Sophan et al. evaluated long-term correction (LTC) parameters that were derived from three Thai reference stations, along with the positioning performance of DFMC SBAS using GPS and Galileo signals. The findings revealed positional errors at the meter level [41], thus highlighting the need for greater regional coverage and system adaptation to fully exploit the benefits of second-generation SBAS in GNSS surveying.

To address these limitations, this research aimed to improve the efficiency of GNSS surveying in Thailand using second-generation SBAS. The approach involved calculating clock and ephemeris corrections based on navigation message data that was collected from a ground tracking network that spanned the entire country and included signals from BDS, GPS, Galileo, and GLONASS satellites. These corrections were then applied to the GNSS survey data using the ionosphere-free combination technique to eliminate ionospheric errors. Finally, data from 20 continuously operating reference stations (CORS) across Thailand were post-processed using the standard point positioning (SPP) method to assess how effectively the corrections improved the positional accuracy.

2. Second-Generation SBAS Information

2.1. Dual-Frequency Multi-Constellation (DFMC) SBAS

DFMC SBAS (known as second-generation SBAS) functions by collecting measurement data from the GNSS through the ground tracking network. This data is then transmitted to a processing station, where the clock and ephemeris corrections are calculated. The corrected data is subsequently stored in a standard SBAS file format and sent to a geostationary satellite (GEO). The GEO then transmits the error correction data in a standardized format to users via the SBAS L5 signal. DFMC SBAS employs ten different message formats, each containing error correction data (with each message consisting of 250 bits). The relationships among these message formats is shown in Figure 1. In addition to generating clock and orbit corrections, second-generation SBAS also incorporates enhanced ionospheric modeling and dual-frequency multi-constellation (DFMC) capabilities; these additions allow it to correct for ionospheric delays more effectively than the earlier systems. Second-generation SBAS provides several notable advantages – especially in terms of improving the efficiency and reliability of GNSS surveying [35, 42–44].

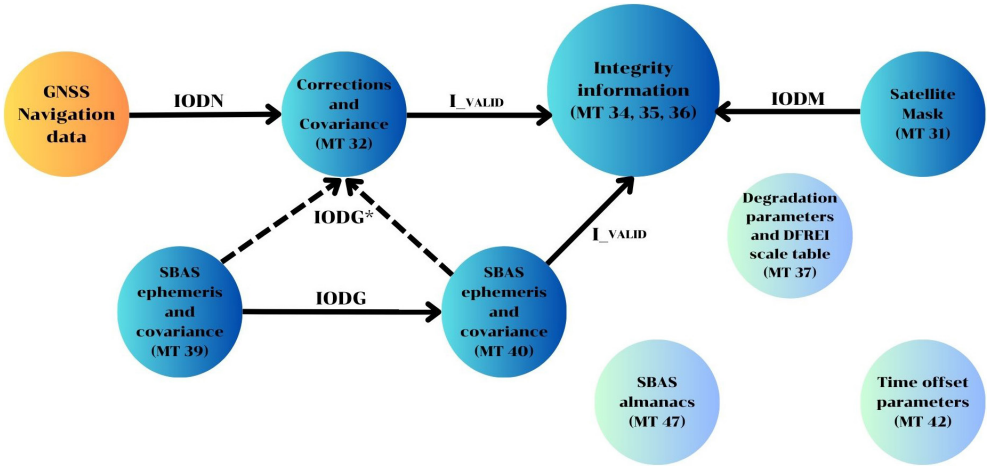

Fig. 1. Relationships among message types:
MT – message type, IODN – issue of data navigation, IODG – issue of data GEO,
IODM – issue of data mask, I_VALID – validity interval,
dashed IODG* – connections between Message Types 39/40 and 32 used when Message Type 32 is transmitted to SBAS satellite

Source: [45]

Second-generation SBAS provides several notable advantages – especially in terms of improving the efficiency and reliability of GNSS surveying [29, 39]. In addition to these core benefits, the system offers the following key features:

- The SBAS Generation 2 system is designed to support a variety of GNSS signals, including those from the Galileo, BeiDou, GLONASS, and GPS constellations. By integrating multiple satellite constellations, the system becomes more robust, thus increasing its ability to resist signal degradation or disruption from any single constellation [40].
- A major improvement in SBAS Generation 2 is the reduction of ionospheric errors – both large in magnitude and geographically specific – in their impacts on surveying. This enhancement extends the system's service area, thereby improving its overall availability and reliability [35].
- With the improved accuracy and reliability of SBAS Generation 2, the need for expensive auxiliary ground infrastructure (such as traditional reference stations) is greatly reduced. This results in cost savings for both the operators and end users while maintaining high performance and safety standards [1, 38].

2.2. International Civil Aviation Organization (ICAO) GNSS Standards for Different Phases of Flight

The ICAO's GNSS standards are crucial for ensuring the safe and efficient operation of aircraft during all phases of flight – particularly as the aviation industry transitions to satellite-based navigation systems.

These standards are outlined in Annex 10 and Doc. 9613 and provide the foundation for modern aviation navigation by ensuring that satellite-based systems meet high standards of accuracy, integrity, availability, and continuity (as shown in Table 1). As the industry increasingly depends on GNSS technology for various operations, these standards will continue to play vital roles. Furthermore, advances in GNSS and enhancement systems such as SBAS are expected to address the evolving needs of aviation, further improving safety and reliability [46, 47].

Table 1. ICAO GNSS standards for different phases of flight

Phases of Flight	Accuracy [m] Integrity		Integrity			Continuity	Availability
	Horizontal	Vertical	Alert limit [m]		Integrity Probability		
			Horizontal	Vertical			
En-route	3700	–	3700	–	$1 - 1 \cdot 10^{-7}$/h	$1 - 10^{-4}$ to $1 - 10^{-8}$/h	0.99–0.99999
Terminal	740	–	1850	–	$1 - 1 \cdot 10^{-7}$/h	$1 - 10^{-4}$ to $1 - 10^{-8}$/h	0.99–0.99999
NPA	220	–	556	–	$1 - 1 \cdot 10^{-7}$/h	$1 - 10^{-4}$ to $1 - 10^{-8}$/h	0.99–0.99999
APV-I	16	20	40	50	$1 - 2 \cdot 10^{-7}$/APCH*	$1 - 8 \cdot 10^{-6}$/15 s	0.99–0.99999
LPV	16	20	40	50	$1 - 2 \cdot 10^{-7}$/APCH	$1 - 8 \cdot 10^{-6}$/15 s	0.99–0.99999
LPV200	16	4	40	35	$1 - 2 \cdot 10^{-7}$/APCH	$1 - 8 \cdot 10^{-6}$/15 s	0.99–0.99999
APV-II	16	8	40	20	$1 - 2 \cdot 10^{-7}$/APCH	$1 - 8 \cdot 10^{-6}$/15 s	0.99–0.99999
CAT-I	16	4–6	40	10–15	$1 - 2 \cdot 10^{-7}$/APCH	$1 - 8 \cdot 10^{-6}$/15 s	0.99–0.99999

* APCH – in any approach.

Source: [46]

3. Methods

3.1. Methodology

Observation model

When evaluating the SBAS satellite system, the second-generation model employs a single-point positioning method that uses pseudo-range data. Furthermore, it reduces ionospheric errors by applying the ionosphere-free combination technique [46].

The corrected pseudo-range for a specific satellite (i) at time k is the following:

$$P_{i,corrected}^{k} = P_{CSC,i}^{k} + TC_{i}^{k} + b_{i}^{k} \tag{1}$$

where:

$P_{CSC,i}$ – the smoothed pseudo-range [m],
TC_i – the tropospheric correction [m],
b_i – the clock correction.

The process of carrier smoothing is described by the following filter:

$$P_{CSC,k} = \alpha P_{meas} + (1-\alpha) P_{proj} \tag{2}$$

$$P_{proj} = P_{CSC,k-1} + \Delta_{carrier\_range} \tag{3}$$

where:

$P_{CSC,k}$ – the smoothed pseudo-range at time k [m],
$P_{CSC,k-1}$ – the previous smoothed pseudo-range at time $k-1$ [m],
α – the filter weighting function (defined as the ratio of the sample interval to the smoothing time constant),
P_{meas} – the measured pseudo-range (as defined in Equation (4)),
$\Delta_{carrier\_range}$ – the change in the carrier range (as defined in Equation (5)).

The measured pseudo-range is calculated using an ionosphere-free combination – a method that effectively removes the impacts of ionospheric errors. By combining data from multiple frequencies, this technique generates a pseudo-range measurement with reduced sensitivity to ionospheric delays, thereby enhancing the accuracy and reliability of the positioning system:

$$P_{meas}^{n,k} = \frac{\gamma_{1,2} P_{1,k} - P_{2,k}}{\gamma_{1,2} - 1} \tag{4}$$

where:

$P_{n,k}$ – the raw pseudo-range of frequency n at time k [m],
$\gamma_{1,2}$ – the square of the ratio of Frequency 1 to Frequency 2.

The carrier range variation is determined using an ionosphere-free combination:

$$\Delta_{carrier\_range}^{k} = \frac{\gamma_{1,2}(\varphi_{1,k} - \varphi_{1,k-1}) - (\varphi_{2,k} - \varphi_{2,k-1})}{\gamma_{1,2} - 1} \tag{5}$$

where:

$\varphi_{n,k}$ – the accumulated carrier for frequency n at time k (the original $\varphi_{n,k}$ has units of cycles, but here they are converted to meters) [m],
$\varphi_{n,k-1}$ – the accumulated carrier for frequency n at time $k-1$ (the original $\varphi_{n,k-1}$ has units of cycles, but here they are converted to meters) [m].

SBAS Navigation Solution

The weighted least-squares navigation solution is represented in the following form (where the measurements are assigned different weights according to their

accuracy); this approach minimizes the weighted sum of the squared residuals, thus ensuring an optimal solution by factoring in the reliability of each data point [46]:

$$\hat{X} = \left(G^T \cdot W \cdot G\right)^{-1} \cdot G^T \cdot W \cdot Y \tag{6}$$

where:

(a) $\hat{X}$ represents the weighted least squares estimate of the error in the user's estimated location.

(b) Y represents a P-dimensional vector that represents the corrected ionosphere-free pseudo-range measurement $P_{i,corrected}$ from Equation (1), subtracted by the expected ranging values, which are derived from the positions of the satellites and the estimated location of the user, where P is the number of satellites used in the navigation solution.

Here, b_i (defined in Equation (1)) represents the clock offset error correction in the SBAS's corrected clock:

$$b_i = c \cdot \delta B_i \tag{7}$$

where c represents the speed of light in a vacuum (299,792,458 m/s), and δB_i represents the SBAS's corrected clock [s].

The satellite position error correction vector with new index is added to the satellite coordinate vector based on the estimated location of the user [46]:

$$\begin{bmatrix} X_{new}(t) \\ Y_{new}(t) \\ Z_{new}(t) \end{bmatrix} = \begin{bmatrix} X(t) \\ Y(t) \\ Z(t) \end{bmatrix} + \begin{bmatrix} \delta X(t) \\ \delta Y(t) \\ \delta Z(t) \end{bmatrix} \tag{8}$$

where $[X(t), Y(t), Z(t)]$ represents the satellite coordinate vector that will be expressed in the WGS-84 ECEF coordinate, and $[\delta X(t), \delta Y(t), \delta Z(t)]$ represents the satellite position correction that will be expressed in the WGS-84 ECEF coordinate.

(c) G is the observation matrix:

$$G_i = \begin{bmatrix} -\cos El_i \cdot \sin Az_i & -\cos El_i \cdot \cos Az_i & -\sin El_i & 1 & n_i \end{bmatrix} \tag{9}$$

where El_i represents the elevation for satellite i after correcting its position, Az_i represents the azimuth for satellite i after correcting its position, and n_i is "1" if the satellite is part of Reference Constellation C2 or "0" if it is part of C1. The term "Reference Constellation" refers to the specific set of satellites used as the basis for applying dual-frequency corrections and evaluating inter-constellation biases. In this context, one constellation (C1) serves as the primary or baseline group of satellites, while the other (C2) is treated as a reference constellation whose measurements are compared against those of C1 to estimate relative corrections or offsets between the two satellite groups.

(d) W is the weighting matrix:

$$W = \begin{bmatrix} w_1 & 0 & \dots & 0 \\ 0 & w_2 & \dots & 0 \\ \vdots & \vdots & \ddots & \vdots \\ 0 & 0 & \dots & w_p \end{bmatrix} \tag{10}$$

where:

$$w_i = \frac{1}{\sigma_i^2} \tag{11}$$

$$\sigma_i^2 = \sigma_{i,DFC}^2 + \sigma_{i,tropo}^2 + \sigma_{i,air,DFC}^2 + \sigma_{i,iono}^2 \tag{12}$$

Here, $\sigma_{i,DFC}^2$ represents the dual-frequency residual error variance (DFC) in the SBAS corrections for satellite i, $\sigma_{i,tropo}^2$ represents the variance of the model for the troposphere residual error for satellite i, $\sigma_{i,air,DFC}^2$ represents the model variance for the combined measurement noise and multipath residual errors that are associated with the ionosphere-free combination of the dual frequency range measurements for satellite i, and $\sigma_{i,iono}^2$ represents the model variance for the residual error without the ionosphere for satellite i.

Protection-Level Calculations

In SBAS, calculating the protection levels involves determining projection matrix S in the context of a general least-squares navigation solution. Projection matrix S is essential, because it defines the relationship between the observed data and the estimated position. By accurately defining S, the system can assess the impacts of the measurement errors, which allows for the calculations of the horizontal- and vertical-protection levels (HPL and VPL) [46]. These protection levels are critical for ensuring the accuracy and reliability of the navigation solution. For a general least squares position solution using two groups of satellites (C1 and C2) the projection matrix S is defined as:

$$S = \begin{bmatrix} S_{east,1} & S_{east,2} & \cdots & S_{east,P} \\ S_{north,1} & S_{north,2} & \cdots & S_{north,P} \\ S_{U,1} & S_{U,2} & \cdots & S_{U,P} \\ S_{t_{C1},1} & S_{t_{C1},2} & \cdots & S_{t_{C1},P} \\ S_{t_{C1C2},1} & S_{t_{C1C2},2} & \cdots & S_{t_{C1C2},P} \end{bmatrix} = (G^T \cdot W \cdot G)^{-1} \cdot G^T \cdot W \tag{13}$$

where:

S – the projection matrix,

$S_{east,P}$ – the partial derivative of position error in the east direction with respect to the pseudorange error on the P^{th} satellite used in the position solution,

$S_{north,P}$ – the partial derivative of position error in the north direction with respect to the pseudorange error on the P^{th} satellite used in the position solution,

$S_{U,P}$ – the partial derivative of position error in the vertical direction with respect to the pseudorange error on the P^{th} satellite used in the position solution,

$S_{t_{C1},P}$ – the partial derivative of the receiver's clock offset with respect to the group C1 reference time on the P^{th} satellite used in the position solution,

$S_{t_{C1C2},P}$ – the partial derivative of time difference observed by the receiver between the signals from group C1 and those from group C2 on the P^{th} satellite used in the position solution,

G – the observation matrix (defined in Equation (9)),

W – the weighting matrix (defined in Equation (10)).

The horizontal-protection levels (HPL) and vertical-protection levels (VPL) will be calculated as follows:

$$HPL = K_H \cdot d_{major} \tag{14}$$

$$VPL = K_{V,PA} \cdot d_U \tag{15}$$

where:

$$K_H = \begin{cases} 6.18 & \text{for en-route through nonprecision approach operations} \\ 6.00 & \text{for APV-I and Category I operations} \end{cases} \text{ [46]},$$

$K_{V,PA} = 5.33$,

PA – precision approach,

d_U – the variance of the model distribution that exceeds the true error distribution along the vertical axis, which is defined as follows:

$$d_u^2 = \sum_{i=1}^{P} S_{U,i}^2 \sigma_i^2 \tag{16}$$

where:

$S_{U,i}$ – the partial derivative of the position error in the vertical direction with respect to the pseudo-range error on the i^{th} satellite,

P – the number of satellites used in the navigation solution,

$\sigma_i^2 = 1/w_i$ (defined in Equation (12)),

d_{major} – the uncertainty in the error along the semimajor axis of the error ellipse is used to calculate the HPL value in Equation (14), which is defined as follows:

$$d_{major} = \sqrt{\frac{d_{east}^2 + d_{north}^2}{2} + \sqrt{\left(\frac{d_{east}^2 + d_{north}^2}{2}\right)^2 + d_{EN}^2}} \tag{17}$$

where:

d^2_{east} – the variance of the model distribution that exceeds the true error distribution along the east axis:

$$d^2_{east} = \sum_{i=1}^{P} S^2_{east,i} \sigma^2_i \tag{18}$$

d^2_{north} – the variance of the model distribution that exceeds the true error distribution along the north axis:

$$d^2_{north} = \sum_{i=1}^{P} S^2_{north,i} \sigma^2_i \tag{19}$$

d^2_{EN} – the covariance of the model distribution along the east and north axes:

$$d^2_{EN} = \sum_{i=1}^{P} S^2_{east,i} S^2_{north,i} \sigma^2_i \tag{20}$$

where:

$S_{east,i}$ – the partial derivative of the position error in the east direction with respect to the pseudo-range error on the i^{th} satellite,

$S_{north,i}$ – the partial derivative of the position error in the north direction with respect to the pseudo-range error on the i_{th} satellite.

3.2. Methods

This study aimed to calculate the correction data of the SBAS Generation 2 system using data from a ground tracking network that was distributed throughout Thailand; the experiments were conducted as described below. Figure 2a shows the locations of the ground tracking network. Survey data that was collected during the periods of January 1–7, April 1–7, August 1–7, and December 1–7, 2023, was used, thus ensuring the representation of all of the seasons in Thailand. The correction data was then calculated in conjunction with a single point location survey using pseudo-range data from 20 CORS stations (which are also distributed in Thailand); this is illustrated in Figure 2b. The data processing has been categorized into three cases as follows:

- Calculate the correction data using the data from a ground tracking network of 4 CORS stations within a 250 km radius of the SBKK station (CKRI, MNSN, ENMA, and SBKK stations).
- Calculate the correction data using the data from a ground tracking network of 8 CORS stations within a 500 km radius of the SBKK station (CKRI, MNSN, ENMA, SBKK, TUTT, TKK1, DSSK, and TPK2 stations).
- Calculate the correction data using the data from a ground tracking network of 12 CORS stations within a radius of more than 500 km from the SBKK station (CKRI, MNSN, ENMA, SBKK, TUTT, TKK1, DSSK, TPK2, PCRI, LMDH, LSN2, and TSKA stations).

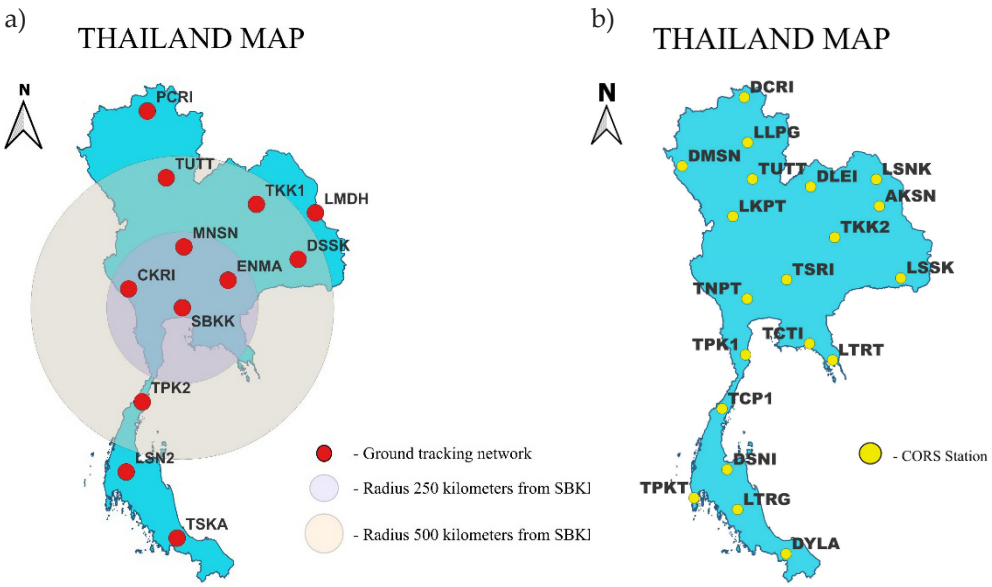

Fig. 2. Ground tracking network generating SBAS corrections (a); CORS stations used to test SBAS corrections (b)

4. Results and Discussion

The positional error values that were derived from the GNSS satellite-positioning system were evaluated in conjunction with the correction data that was generated by the SBAS Generation 2 system (which computed corrections based on the data from a ground tracking network that was distributed throughout Thailand). The evaluation process began with the calculations of the correction values using the data from an initial set of four ground tracking stations, followed by gradual increases to 8 and 12 stations. The test was carried out over four periods in 2023 (January 1–7, April 1–7, August 1–7, and December 1–7) using survey data from 20 CORS stations that were strategically distributed throughout the country.

Table 2 shows the vertical- and horizontal-position errors of the GNSS satellite-positioning system after being processed with the correction data that was generated by the SBAS Generation 2 system for each CORS station. The analysis showed that, when the SBAS corrections that were based on the four-station ground tracking network were applied, the average horizontal- and vertical-position errors were 1.85 m and 2.43 m, respectively, at the 20 CORS stations (with a confidence level of 95%). Similarly, when the corrections that were derived from the network of 8 stations were used, the average horizontal- and vertical-position errors remained 1.60 m and 2.25 m, respectively, at the same confidence level. Furthermore, the application of the SBAS corrections from the network of 12 stations produced similar results,

with average horizontal- and vertical-position errors again being recorded at 1.51 m and 2.24 m, respectively (at a 95% confidence level). However, a statistical analysis showed that the differences in the position errors between the 8- and 12-station configurations were not statistically significant at the 95% confidence level. Figures 3 and 4 illustrate the data using bar charts to enhance comparability.

Table 2. Positional-error testing with SBAS Generation 2 system in GNSS satellite positioning

Positioning errors at each CORS station	4 Ground Tracking Network		8 Ground Tracking Network		12 Ground Tracking Network	
	HPE [m] (95% CI)	VPE [m] (95% CI)	HPE [m] (95% CI)	VPE [m] (95% CI)	HPE [m] (95% CI)	VPE [m] (95% CI)
1. AKSN	1.80	2.44	1.72	2.60	1.65	2.62
2. DCRI	1.69	2.14	1.58	1.90	1.58	2.07
3. DLEI	1.88	2.28	1.61	2.13	1.52	2.15
4. DMSN	1.89	2.28	1.42	2.12	1.51	2.10
5. DSNI	1.76	2.40	1.55	2.13	1.47	2.17
6. DYLA	1.75	2.46	1.27	2.17	1.61	2.20
7. LKPT	1.83	2.48	1.52	2.50	1.50	2.35
8. LLPG	1.85	2.56	1.50	2.41	1.41	2.18
9. LSNK	1.74	2.44	1.55	2.21	1.44	2.20
10. LSSK	1.88	2.52	1.77	2.29	1.51	2.25
11. LTRG	1.87	2.39	1.73	2.31	1.74	2.27
12. LTRT	1.89	2.56	1.60	2.32	1.44	2.34
13. TCP1	1.76	2.58	1.71	2.03	1.51	2.10
14. TCTI	1.93	2.07	1.46	2.20	1.53	2.18
15. TNPT	1.78	2.54	1.48	2.24	1.50	2.23
16. TPK1	1.89	2.59	1.72	2.40	1.33	2.42
17. TPKT	1.84	2.52	1.78	2.25	1.52	2.22
18. TSRI	1.81	2.57	1.77	2.40	1.53	2.37
19. TUTT	1.86	2.33	1.51	2.25	1.48	2.15
20. TKK2	1.80	2.41	1.67	2.18	1.49	2.14
Average	1.85	2.43	1.60	2.25	1.51	2.24

Note: HPE stands for horizontal-positioning error, VPE stands for vertical-positioning error, and 95% CI stands for 95% confidence interval.

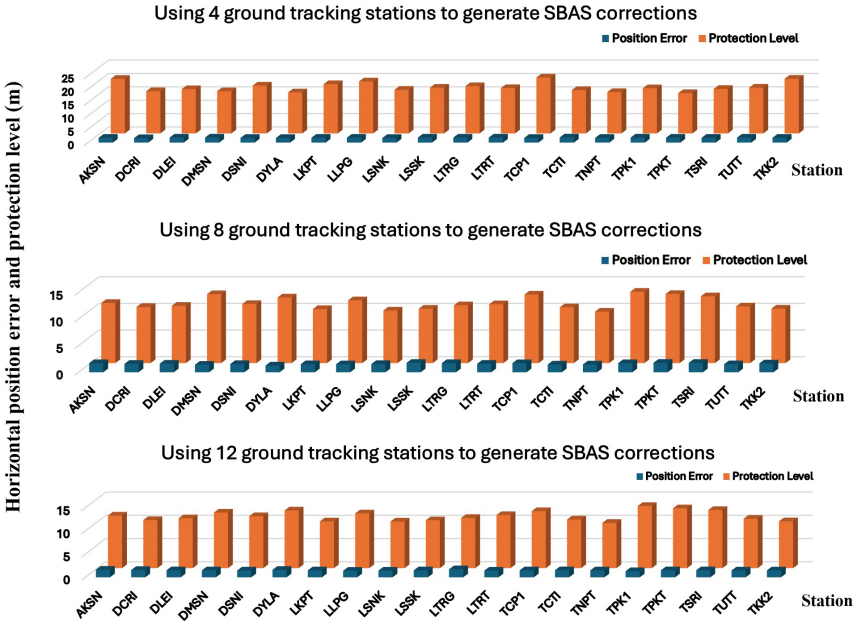

Fig. 3. Comparison of horizontal-position errors and protection-level values across CORS stations

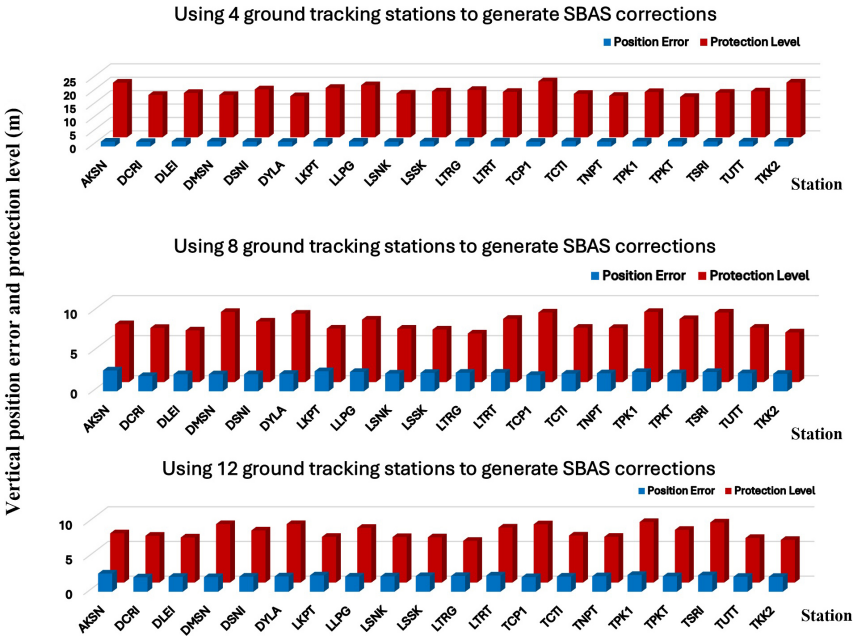

Fig. 4. Comparison of vertical-position errors and protection-level values across CORS stations

Figures 5 and 6 illustrate the test results from the TSRI station – one of the 20 CORS stations that were included in this study. The graph shows the relationship among the vertical- and horizontal-position errors and the protection-level values for four distinct periods: January 1–7 (Day of Year: 1–7), April 1–7 (DoY: 91–97), August 1–7 (DoY: 213–219) and December 1–7 (DoY: 335–341), 2023. The results revealed that the horizontal- and vertical-position errors remained consistently below the protection levels throughout the test when using the SBAS correction data that was derived from the ground tracking networks of 8 and 12 stations (see Table 3). Furthermore, the analysis confirmed that both the vertical- and horizontal-position errors as well as the protection-level values met the Category I (CAT-I) flight requirements that are outlined by the ICAO standards when the networks of 8 and 12 receivers were used for the SBAS correction calculations. During certain periods, however, the horizontal- and vertical-position errors (along with the protection-level values) exceeded the Category I (CAT-I) flight standards when the network of four receivers was employed. The protection level served as a key indicator of the performance of the SBAS system and its compliance with the ICAO standards.

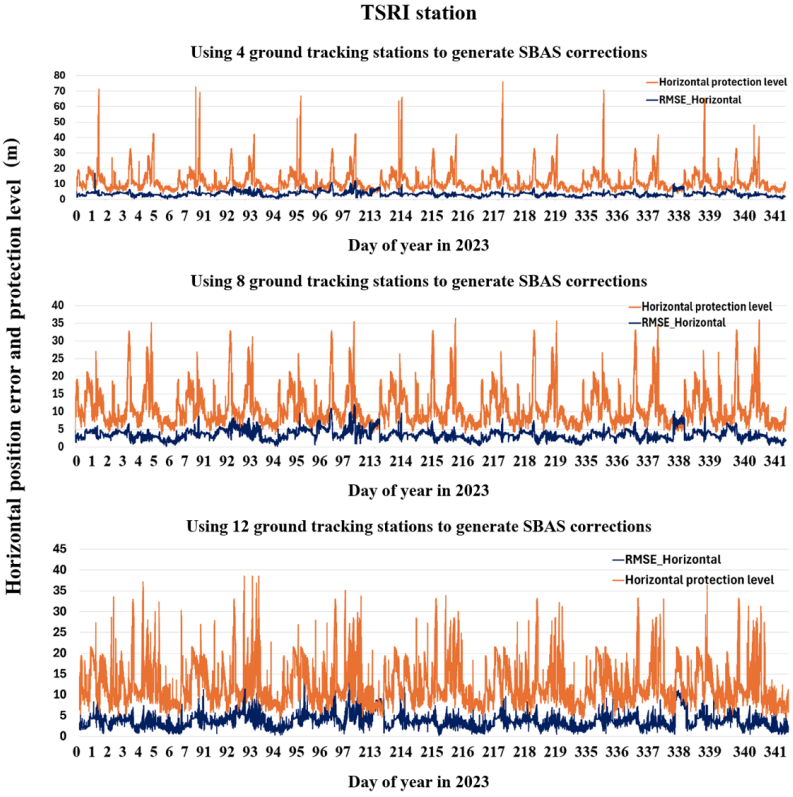

Fig. 5. Relationships between horizontal-position errors and protection-level values at TSRI station

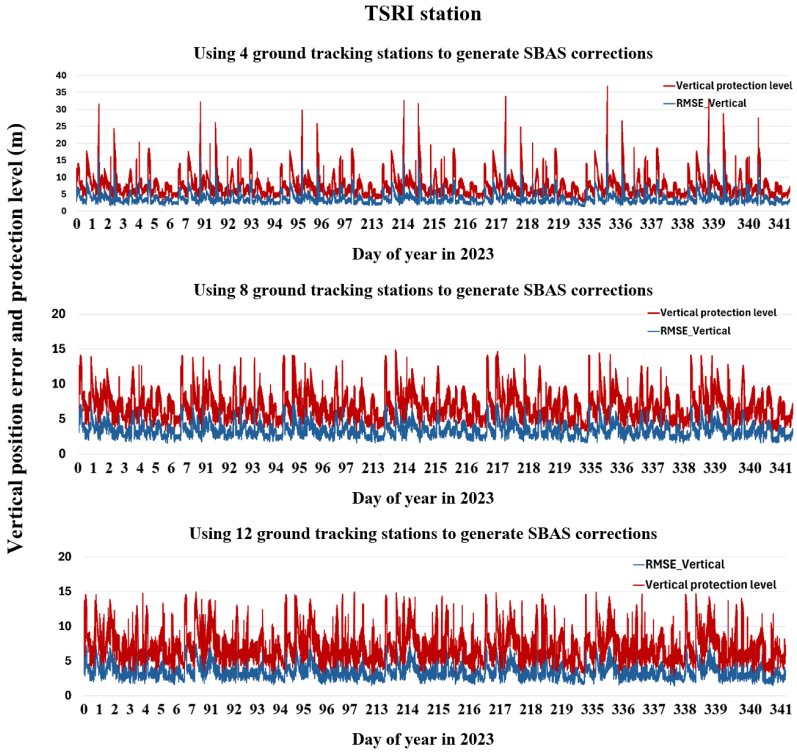

Fig. 6. Relationships between vertical-position errors and protection-level values at TSRI station

Table 3. Protection-level testing with SBAS Generation 2 system in GNSS satellite positioning

Protection level at each CORS station	4 Ground Tracking Network		8 Ground Tracking Network		12 Ground Tracking Network	
	HPL [m] (95% CI)	VPL [m] (95% CI)	HPL [m] (95% CI)	VPL [m] (95% CI)	HPL [m] (95% CI)	VPL [m] (95% CI)
1. AKSN	20.38	15.79	11.29	7.23	11.34	7.10
2. DCRI	15.79	11.53	10.54	6.76	10.36	6.75
3. DLEI	16.54	15.31	10.76	6.45	10.75	6.50
4. DMSN	15.77	10.85	12.94	8.76	11.97	8.43
5. DSNI	17.87	11.30	11.09	7.56	11.20	7.51
6. DYLA	15.33	12.87	12.32	8.54	12.43	8.43
7. LKPT	18.42	16.43	10.14	6.68	10.08	6.59

Table 3. cont.

Protection level at each CORS station	4 Ground Tracking Network		8 Ground Tracking Network		12 Ground Tracking Network	
	HPL [m] (95% CI)	VPL [m] (95% CI)	HPL [m] (95% CI)	VPL [m] (95% CI)	HPL [m] (95% CI)	VPL [m] (95% CI)
8. LLPG	19.43	12.53	11.79	7.80	11.80	7.89
9. LSNK	16.31	14.67	9.87	6.67	10.05	6.56
10. LSSK	17.09	10.98	10.21	6.56	10.32	6.52
11. LTRG	17.67	15.54	10.85	6.07	10.82	6.01
12. LTRT	16.93	10.13	11.04	7.90	11.44	7.93
13. TCP1	20.87	13.67	12.87	8.69	12.29	8.40
14. TCTI	16.21	13.29	10.47	6.78	10.48	6.78
15. TNPT	15.45	10.87	9.66	6.76	9.76	6.60
16. TPK1	16.87	11.27	13.39	8.76	13.39	8.73
17. TPKT	15.05	12.03	12.97	7.87	12.90	7.60
18. TSRI	16.62	11.76	12.54	8.68	12.53	8.66
19. TUTT	17.11	15.02	10.64	6.79	10.65	6.43
20. TKK2	20.42	13.12	10.23	6.20	10.10	6.15
Average	17.31	12.95	11.28	7.38	11.23	7.28

Note: HPL stands for horizontal-protection level, VPL stands for vertical-protection level, and 95% CI stands for 95% confidence interval.

5. Conclusions and Future Work

In conclusion, this study demonstrated that the SBAS Generation 2 system can significantly improve the accuracy and reliability of GNSS-based positioning systems when implemented with an appropriate network of ground tracking stations, thereby meeting ICAO's Category I standards for aviation. The results also suggested that increasing the number of ground tracking stations improved the overall performance of the system, thus ensuring compliance with stringent flight-safety standards. This preliminary study lays the foundation for the ongoing development of a full-scale SBAS Generation 2 service that is tailored to meet Thailand's needs. Future research could focus on optimizing the balance among coverage, performance, and costs, further advancing the practical application of the SBAS system in aviation. In addition, future work could examine the computational costs and

operational feasibility of scaling a national SBAS service – particularly in terms of infrastructure requirements, real-time data processing demands, and long-term sustainability.

Funding

This research received no specific grant from any funding agency in the public, commercial, or not-for-profit sectors.

CRediT Author Contribution

P. T.: conceptualization, methodology, software, validation, formal analysis, investigation, resources, data curation, writing – original draft preparation, visualization.

C. S.: conceptualization, validation, writing – review and editing, supervision, project administration.

Declaration of Competing Interests

The authors declare that they have no known competing financial interests or personal relationships that could have appeared to influence the work reported in this paper.

Data Availability

No data.

Use of Generative AI and AI-Assisted Technologies

No generative AI or AI-assisted technologies were employed in the preparation of this manuscript.

Acknowledgement

We would like to acknowledge the Royal Thai Survey Department for providing the GNSS observation data that was used in this research.

References

[1] Gao W., Cao Y., Liu C., Lu J., Shao B., Xiong S., Su C.: *Construction progress and aviation flight test of BDSBAS.* Remote Sensing, vol. 14(5), 2022, 1218. https://doi.org/10.3390/rs14051218.

[2] Pringvanich N., Satirapod C.: *SBAS algorithm performance in the implementation of the ASIAPACIFIC GNSS test bed.* The Journal of Navigation, vol. 60(3), 2007, pp. 363–371. https://doi.org/10.1017/S0373463307004274.

[3] Zheng S., Gao M., Huang Z., Jin X., Li K.: *Satellite integrity monitoring for satellite-based augmentation system: An improved covariance-based method.* Satellite Navigation, vol. 3(1), 2022, 9. https://doi.org/10.1186/s43020-022-00070-6.

[4] Dautermann T.: *Civil air navigation using GNSS enhanced by wide area satellite based augmentation systems.* Progress in Aerospace Sciences, vol. 67, 2014, pp. 51–62. https://doi.org/10.1016/j.paerosci.2014.01.003.

[5] Heßelbarth A., Wanninger L.: *SBAS orbit and satellite clock corrections for precise point positioning.* GPS Solutions, vol. 17, 2013, pp. 465–473. https://doi.org/10.1007/s10291-012-0292-6.

[6] Hu Z., Liu X., Wang G., Zhang Q., Zhou R., Chen L., Zhao Q.: *Initial performance assessment of the single-frequency (SF) service with the BeiDou satellite-based augmentation system (BDSBAS).* GPS Solutions, vol. 27(1), 2023, 35. https://doi.org/10.1007/s10291-022-01372-7.

[7] Pringvanich N., Satirapod C.: *Flight test results and analysis of SBAS-like algorithm from the implementation of the Asia-Pacific GNSS test bed.* The Aeronautical Journal, vol. 113(1139), 2009, pp. 35–40.

[8] Arnold L.L., Zandbergen P.A.: *Positional accuracy of the wide area augmentation system in consumer-grade GPS units.* Computers & Geosciences, vol. 37(7), 2011, pp. 883–892. https://doi.org/10.1016/j.cageo.2010.12.011.

[9] El-Arini M. B., Poor W., Lejeune R., Conker R., Fernow J., Markin K.: *An introduction to Wide Area Augmentation System and its predicted performance.* Radio Science, vol. 36(5), 2001, pp. 1233–1240. https://doi.org/10.1029/1999RS002426.

[10] Gauthier L., Michel P., Ventura-Traveset J., Benedicto J.: *EGNOS: The first step in Europe's contribution to the global navigation satellite system.* ESA Bulletin, vol. 105, 2001, pp. 35–42.

[11] Li X., Fang K., Wang H., Wang S., Wang Z.: *Evaluation for BDSBAS single-frequency service assisted by data authentication*, [in:] *Proceedings of the 2025 International Technical Meeting of The Institute of Navigation*, Long Beach, California, January 2025, pp. 590–603. https://doi.org/10.33012/2025.19979.

[12] Nandulal S., Rao C.B., Indi C.L., Irulappan M., Arulmozhi S., Soma P.: *Evaluation of real-time position accuracy and LNAV/VNAV service availability of GAGAN SBAS (Wide Area Differential GPS) over Indian region*, [in:] *2008 Tyrrhenian International Workshop on Digital Communications – Enhanced Surveillance of Aircraft and Vehicles*, IEEE, 2008, pp. 1–6. https://doi.org/10.1109/TIWDC.2008.4649025.

[13] Suryanarayana Rao K.N.: *GAGAN – The Indian satellite based augmentation system.* Indian Journal of Radio and Space Physics, vol. 36(4), 2007, pp. 293–302.

[14] Thari P., Thongtan T., Satirapod C.: *GNSS positioning accuracy performance assessments on 1st and 2nd generation SBAS signals in Thailand.* Journal of Applied Geodesy, vol. 18(3), 2024. pp. 421–431. https://doi.org/10.1515/jag-2023-0082.

[15] Goswami M., Mahato S., Ghatak R., Bose A.: *Potential of satellite-based augmentation systems (SBAS) in test and evaluation of missiles in Indian test range applications*. Journal of the Indian Society of Remote Sensing, vol. 51(12), 2023, pp. 2537–2547. https://doi.org/10.1007/s12524-023-01787-w.

[16] Dammalage T., De Silva D.N., Satirapod C.: *Performance analysis of GPS aided geo augmented navigation (GAGAN) over Sri Lanka.* Engineering Journal, vol. 21(5), 2017, pp. 305–314. https://doi.org/10.4186/ej.2017.21.5.305.

[17] Pungpet P., Kitpracha C., Promchot D., Satirapod C.: *Positioning accuracy analyses on GPS single point positioning determination with GAGAN correction services in Thailand*, [in:] *2018 15th international conference on electrical engineering/electronics, computer, telecommunications and information technology (ECTI-CON)*, IEEE, 2018, pp. pp. 724–727. https://doi.org/10.1109/ECTICon.2018.8619969.

[18] Thari P., Kriengkraiwasin S., Satirapod C.: *Evaluation of GNSS positioning accuracy from satellite-based augmentation systems in Thailand.* Engineering & Applied Science Research, vol. 49(2), 2022, pp. 209–217. https://doi.org/10.14456/easr.2022.23.

[19] Barrios J., Pericacho J.G., Domenech G., López N.A.: *Worldwide SBAS broadcasts between 2017 and 2022: A comparative study*, [in:] *Proceedings of the 35th International Technical Meeting of the Satellite Division of The Institute of Navigation (ION GNSS+ 2022)*. Denver, Colorado 2022, pp. 117–153. https://doi.org/10.33012/2022.18356.

[20] Charoenkalunyuta T., Satirapod C.: *Effect of Thai ionospheric maps (THIM) model on the performance of network based RTK GPS in Thailand*. Survey Review, vol. 46(334), 2014, pp. 1–6. https://doi.org/10.1179/1752270613Y.0000000055.

[21] Tsujii T., Fujiwara T., Kubota T., Satirapod C., Supnithi P., Tsugawa T., Lee H.: *Measurement and simulation of equatorial ionospheric plasma bubbles to assess their impact on GNSS performance.* Journal of the Korean Society of Surveying, Geodesy, Photogrammetry and Cartography, vol. 30(6_2), 2012, pp. 607–613.

[22] Prakanrattana K., Satirapod C.: *Comparative study of using different ionosphere models in Thailand for single-frequency GNSS users*. Survey Review, vol. 51(366), 2019, pp. 213–218. https://doi.org/10.1080/00396265.2018.1426260.

[23] Ma G., Hocke K., Li J., Wan Q., Lu W., Fu W.: *GNSS ionosphere sounding of equatorial plasma bubbles*. Atmosphere, vol. 10(11), 2019, 676. https://doi.org/10.3390/atmos10110676.

[24] Balan N., Liu L., Le H.: *A brief review of equatorial ionization anomaly and ionospheric irregularities*. Earth and Planetary Physics, vol. 2(4), 2018, pp. 257–275.

[25] Luo X., Wang D., Wang J., Wu Z., Gao J., Zhang T., Yang C., Qin X., Chen X.: *Study of the spatiotemporal characteristics of the equatorial ionization anomaly using shipborne multi-GNSS data: a case analysis (120–150°E, Western Pacific Ocean, 2014–2015)*. Remote Sensing, vol. 13(15), 2021, 3051. https://doi.org/10.3390/rs13153051.

[26] Sophan S., Myint L. M., Saito S., Supnithi P.: *Performance improvement of the GAGAN satellite-based augmentation system based on local ionospheric delay estimation in Thailand*. GPS Solutions, vol. 26(4), 2022, 130. https://doi.org/10.1007/s10291-022-01293-5.

[27] Liu Y., Cao Y., Tang C., Chen J., Zhao L., Zhou S., Hu X., Tian Q., Yang Y.: *Pseudorange bias analysis and preliminary service performance evaluation of BDSBAS*. Remote Sensing, vol. 13(23), 2021, 4815. https://doi.org/10.3390/rs13234815.

[28] Netthonglang C., Thongtan T., Satirapod C.: *GNSS precise positioning determinations using smartphones*, [in:] *2019 IEEE Asia Pacific Conference on Circuits and Systems (APCCAS)*, IEEE, 2019, pp. 401–404. https://doi.org/10.1109/APCCAS47518.2019.8953132.

[29] Yang Y., Ding Q., Gao W., Li J., Xu Y., Sun B.: *Principle and performance of BDSBAS and PPP-B2b of BDS-3*. Satellite Navigation, vol. 3(1), 2022, 5. https://doi.org/10.1186/s43020-022-00066-2.

[30] Cao Y., Chen J., Liu L., Hu X., Liu Y., Xin J., Zhao L., Tian Q., Zhao S., Wu B.: *Development status and service performance preliminary analysis for BDSBAS*. Remote Sensing, vol. 14(17), 2022, 4314. https://doi.org/10.3390/rs14174314.

[31] Schlüter S., Hoque M.M.: *An SBAS integrity model to overbound residuals of higher-order ionospheric effects in the ionosphere-free linear combination*. Remote Sensing, vol. 12(15), 2020, 2467. https://doi.org/10.3390/rs12152467.

[32] Mahato S., Santra A., Dan S., Verma P., Banerjee P., Bose A.: *Visibility anomaly of GNSS satellite and support from regional systems*. Current Science, vol. 119(11), 2020, pp. 1774–1782. https://doi.org/10.18520/cs/v119/i11/1774-1782.

[33] El-Mowafy A., Cheung N., Rubinov E.: *First results of using the second generation SBAS in Australian urban and suburban road environments*. Journal of Spatial Science, vol. 65(1), 2020, pp. 99–121. https://doi.org/10.1080/14498596.2019.1664943.

[34] Wang K., El-Mowafy A., Khaki M., Sutherland T., Rubinov E.: *Assessment of the new DFMC and PPP services of the second-generation SBAS in the mining and urban environments*, [in:] *Proceedings of International Global Navigation Satellite Systems Symposium (IGNSS 2020), 5–7 February 2020, Sydney, Australia*, 2020, pp. 1–15. https://espace.curtin.edu.au/handle/20.500.11937/79701.

[35] Wu J., Wang K., El-Mowafy A.: *Preliminary performance analysis of a prototype DFMC SBAS service over Australia and Asia-Pacific*. Advances in Space Research, vol. 66(6), 2020, pp. 1329–1341. https://doi.org/10.1016/j.asr.2020.05.026.

[36] Shao B., Ding Q., Wu X.: *Estimation method of SBAS dual-frequency range error integrity parameter*. Satellite Navigation, vol. 1(1), 2020, 9. https://doi.org/10.1186/s43020-020-00011-1.

[37] Wang X., Cui X., Wei K., Liu G., Gao Y., Lu M.: *Signal quality monitoring algorithms of DFMC SBAS for dual-frequency civil signals of BDS*, [in:] Yang C., Xie J. (eds.), *China Satellite Navigation Conference (CSNC 2021) Proceedings: Volume II*, Lecture Notes in Electrical Engineering, vol. 773, Springer, Singapore 2021, pp. 75–91. https://doi.org/10.1007/978-981-16-3142-9_8.

[38] Liu Y., Cao Y., Shao B., Tang C., Zhou S., Hu X., Yang J., Liu J., Li P.: *Research on performance improvement method of BDSBAS multi-GNSS service with DFMC protocol*. Advances in Space Research, vol. 72(6), 2023, pp. 2283–2296. https://doi.org/10.1016/j.asr.2023.06.024.

[39] Wang Z., Wang L., Xie W., Huang G., Yang W., Tian Y.: *DFMC SBAS service performance analysis of multi-GNSS based on BDS-3 in different regions*. Measurement Science and Technology, vol. 35(11), 2024, 116310. https://doi.org/10.1088/1361-6501/ad6f38.

[40] Zhao L., Hu X., Tang C., Cao Y., Zhou S., Yang Y., Liu L., Guo R.: *Generation of DFMC SBAS corrections for BDS-3 satellites and improved positioning performances*. Advances in Space Research, vol. 66(3), 2020, pp. 702–714. https://doi.org/10.1016/j.asr.2020.04.032.

[41] Sophan S., Myint L.M., Supnithi P.: *Preliminary evaluations of user positioning errors in DFMC SBAS demo at Thailand location*, [in:] *Proceedings of International Workshop on ATM/CNS 2022*, Electronic Navigation Research Institute, Tokyo 2022, pp. 49–54. https://doi.org/10.57358/iwac.1.0_49.

[42] Barrios J., Caro J., Calle J.D., Carbonell E., Pericacho J.G., Fernández G., Esteban V.M., Fernández M.A., Bravo F., Torres B., Calabrese A., Diaz A., Rodríguez I., Laínez M.D., Romay M.M., Jackson R., Reddan R.E., Bunce D., Soddu C.: *Update on Australia and New Zealand DFMC SBAS and PPP system results*, [in:] *Proceedings of the 31st International Technical Meeting of the Satellite Division of The Institute of Navigation (ION GNSS+ 2018)*, Institute of Navigation, 2018, pp. 1038–1067. https://doi.org/10.33012/2018.15932.

[43] Cheng L., Weiguang G., Bo S., Jun L., Wei W., Ying C., Chengeng S., Shuai X., Qun D.: *Development of BeiDou satellite-based augmentation system*. Navigation, vol. 68(2), 2021, pp. 405–417. https://doi.org/10.1002/navi.422.

[44] Wang X., Cui X., Liu G., Lu M.: *Designing the signal quality monitoring algorithm based on chip domain observables for BDS B1C/B2a signals under the requirements of DFMC SBAS*, Remote Sensing, vol. 15(4), 2023, 1008. https://doi.org/10.3390/rs15041008.

[45] EUROCAE: *ED-259A: Minimum Operational Performance Standard for Dual-Frequency Multi-Constellation Satellite-Based Augmentation System Airborne Equipment*. European Organization for Civil Aviation Equipment, Saint-Denis, France 2023.

[46] ICAO: *Annex 10 to the Convention on International Civil Aviation: Aeronautical Telecommunication. Volume I: Radio Navigation Aids*. 7th ed. International Civil Aviation Organization, Montréal, Quebec, Canada 2018.

[47] ICAO.: *Doc 9613: Performance-based Navigation (PBN) Manual*. 5th ed. International Civil Aviation Organization, Montreal 2023.